ARTICLES

Cytosporone B is an agonist for nuclear orphan receptor Nur77

Yanyan Zhan[1,3], Xiping Du[1,3], Hangzi Chen[1], Jingjing Liu[1], Bixing Zhao[1], Danhong Huang[1], Guideng Li[1], Qingyan Xu[1], Mingqing Zhang[1], Bart C Weimer[2], Dong Chen[2], Zhe Cheng[1], Lianru Zhang[1], Qinxi Li[1], Shaowei Li[1], Zhonghui Zheng[1], Siyang Song[1], Yaojian Huang[1], Zhiyun Ye[1], Wenjin Su[1], Sheng-Cai Lin[1], Yuemao Shen[1] & Qiao Wu[1]

Nuclear orphan receptor Nur77 has important roles in many biological processes. However, a physiological ligand for Nur77 has not been identified. Here, we report that the octaketide cytosporone B (Csn-B) is a naturally occurring agonist for Nur77. Csn-B specifically binds to the ligand-binding domain of Nur77 and stimulates Nur77-dependent transactivational activity towards target genes including *Nr4a1* (*Nur77*) itself, which contains multiple consensus response elements allowing positive autoregulation in a Csn-B–dependent manner. Csn-B also elevates blood glucose levels in fasting C57 mice, an effect that is accompanied by induction of multiple genes involved in gluconeogenesis. These biological effects were not observed in Nur77-null (*Nr4a1*$^{-/-}$) mice, which indicates that Csn-B regulates gluconeogenesis through Nur77. Moreover, Csn-B induced apoptosis and retarded xenograft tumor growth by inducing Nur77 expression, translocating Nur77 to mitochondria to cause cytochrome *c* release. Thus, Csn-B may represent a promising therapeutic drug for cancers and hypoglycemia, and it may also be useful as a reagent to increase understanding of Nur77 biological function.

Nuclear receptors play important roles in numerous biological processes, including cell proliferation, differentiation, apoptosis, metabolism and development[1,2]. They constitute an important group of molecules for drug targets as well. The orphan receptors, Nur77 (also known as TR3, NGFI-B, TIS1 and NAK-1), Nurr1 (RNR-1, TINUR and HZF-3) and NOR1 (MINOR, CHN and TEC), belong to the nuclear receptor subfamily 4 group A (NR4A)[3,4], which act as transcription factors to regulate the expression of target genes by targeting their response elements[5,6].
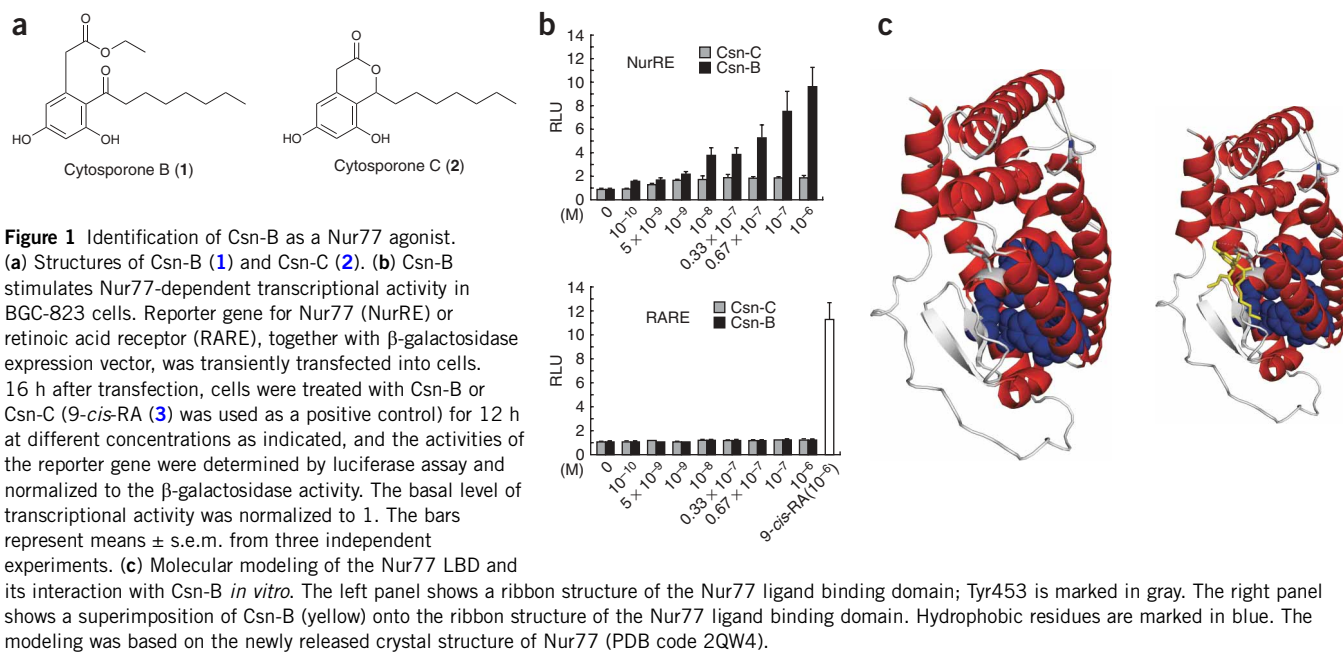
A role for Nur77 in apoptosis was first reported in 1994—Nur77 mRNA was shown to be induced by T-cell receptor signaling, and Nur77 was shown to be required for T-cell receptor-mediated apoptosis[7,8]. Overexpression of a dominant-negative Nur77 or knockdown of Nur77 expression by antisense RNA inhibited T-cell receptor-induced apoptosis[7,8]. The closely related orphan receptor NOR1 also plays a key role in apoptosis of T lymphocytes, eosinophils and various other cell types[9,10]. Additionally, in response to apoptosis stimuli, Nur77 migrates from the nucleus to the cytoplasm where it directly targets the mitochondria to initiate cell apoptosis[11,12]. Notably, retinoid X receptor α (RXRα) acts as a carrier to assist Nur77 translocation from the nucleus to the mitochondria in the presence of 9-*cis*-retinoic acid, an RXR ligand. In the mitochondria, Nur77 (not RXRα) causes the release of cytochrome *c* (ref. 13).

Recently, it has been reported that Nur77, along with two other subfamily members (Nurr1 and NOR1), has a critical role in glucose homeostasis. Adenoviral expression of Nur77 induces genes involved in gluconeogenesis, stimulates glucose production and raises blood glucose levels[14]. Nur77 is a positive regulator of *G6pc*, *Fbp1*, *Fbp2* and *Eno3*, which act to increase the glucose pool for hepatic output. Overexpression of NOR1 also increases insulin-augmented glucose transport in 3T3-L1 adipocytes[15]. It is conceivable that increased sensitivity of insulin may be a consequence of increased blood glucose levels[15]. Though much remains to be clarified as to how NOR1 regulates glucose homeostasis, these findings indicate that the Nur77 homolog NOR1 also plays an important role in regulating blood glucose levels. One may hypothesize that the NR4A subfamily members are potential targets for treatment of metabolic diseases.

As with other nuclear receptors, Nur77 has common structural features with an N-terminal domain that contains an activation function 1 (AF-1), a DNA binding domain (DBD), a C-terminal domain that contains the ligand binding domain (LBD), and a ligand-dependent transcriptional activation domain, AF-2 (ref. 16). However, a physiological ligand for Nur77 has not been identified. Structural analysis of the putative ligand binding domain of Nurr1 and the *Drosophila melanogaster* ortholog of NOR1 reveals a ligand binding pocket in these receptors, although one study suggests that the putative ligand pocket is blocked by side chains from six different

Figure 1 Identification of Csn-B as a Nur77 agonist. (a) Structures of Csn-B (1) and Csn-C (2). (b) Csn-B stimulates Nur77-dependent transcriptional activity in BGC-823 cells. Reporter gene for Nur77 (NurRE) or retinoic acid receptor (RARE), together with β-galactosidase expression vector, was transiently transfected into cells. 16 h after transfection, cells were treated with Csn-B or Csn-C (9-cis-RA (3) was used as a positive control) for 12 h at different concentrations as indicated, and the activities of the reporter gene were determined by luciferase assay and normalized to the β-galactosidase activity. The basal level of transcriptional activity was normalized to 1. The bars represent means ± s.e.m. from three independent experiments. (c) Molecular modeling of the Nur77 LBD and its interaction with Csn-B *in vitro*. The left panel shows a ribbon structure of the Nur77 ligand binding domain; Tyr453 is marked in gray. The right panel shows a superimposition of Csn-B (yellow) onto the ribbon structure of the Nur77 ligand binding domain. Hydrophobic residues are marked in blue. The modeling was based on the newly released crystal structure of Nur77 (PDB code 2QW4).

residues[17–19]. Previous studies found that synthetic compounds known as DIMs act as agonists to stimulate the pro-apoptotic functions of Nur77 directly at the transcriptional level[20,21]. However, some of the pro-apoptotic effects of DIMs are receptor independent[21], which suggests that there may not be a physical interaction between the DIMs and Nur77.

We are interested in the regulation of Nur77 and in identifying naturally occurring compounds that alter Nur77 functions, especially those related to its ability to modulate transactivational activity and apoptosis. In the present study, we identified the octaketide Csn-B (ref. 22), which was isolated from *Dothiorella* sp. HTF3, an endophytic fungus, to be a naturally occurring agonist for Nur77. Csn-B has a strong affinity for Nur77 and stimulates the transactivational activity of Nur77. Moreover, Csn-B increases Nur77-mediated induction of apoptosis, increases growth inhibition of xenograft tumors in nude mice, and enhances gluconeogenesis in mouse liver. Importantly, Csn-B did not exert any of these effects in Nur77-null mice or cells. These lines of evidence not only indicate that Csn-B indeed acts as an agonist for Nur77, but also reveal that Csn-B may be useful in the development of new therapeutic drugs to treat cancer and hypoglycemia.

RESULTS
Identification of Csn-B as an agonist for Nur77
To identify potential Nur77 agonists, a bank of natural products isolated from endophytic fungi was screened using a luciferase-linked Nur77 reporter gene containing an Nur response element (NurRE)[5]. We discovered that the octaketide Csn-B (1)[22] (**Fig. 1a**) stimulates Nur77-dependent transcriptional activity (**Fig. 1b**). However, this was not observed in cytosporone C (Csn-C, 2), a structurally related derivative (**Fig. 1a,b**). Csn-B stimulated the transcriptional activation of the NurRE reporter gene in a dose-dependent manner in gastric cancer cells BGC-823 (**Fig. 1b**), whereas it had no influence on the transcription of reporter genes for the retinoic acid receptor response element (RARE) (**Fig. 1b**), estrogen receptor response element (ERE) or thyroid receptor response element (TRE) (**Supplementary Fig. 1** online), thus indicating target specificity.

We next used molecular modeling with the crystal structure of Nur77 to analyze whether Csn-B can bind to Nur77. By superimposing the Csn-B structure onto the predicted ligand binding domain (**Fig. 1c**) to determine the possible bonding partners, we observed one hydrogen bond between Csn-B and the hydroxyl group of Tyr453 (**Fig. 1c**). In addition to the hydrogen bonding of the aromatic head of Csn-B, the alkyl tail may form hydrophobic interactions with the hydrophobic residues that were aligned on the surface of the ligand binding domain of Nur77. Therefore, this molecular modeling revealed that Tyr453 is situated on the surface of a pocket. More importantly, the six hydrophobic residues (**Fig. 1c**) that were believed to block the putative ligand binding pocket in both Nurr1 and NOR1 (refs. 17,18) were buried interior to the pocket in Nur77.

Csn-B physically binds to Nur77
The molecular modeling of Nur77 proposed above infers a physical binding of Csn-B to Nur77 (see **Fig. 2a** for a map of Nur77 domains). We thus tested this possibility with a number of methods. First, we determined the physical interaction between this compound and Nur77 by fluorescence quenching analysis. Glutathione S-transferase (GST)-Nur77 displayed maximal fluorescence at 336 nm (**Fig. 2b**), whereas Csn-B itself had no fluorescence at this wavelength (**Supplementary Fig. 2a** online). When the GST-Nur77 protein was incubated with increasing amounts of Csn-B, the fluorescence intensity gradually decreased (**Fig. 2b**), whereas Csn-C did not have such an effect (**Supplementary Fig. 2b** online). We then determined which domain of Nur77 is involved in Csn-B binding by generating truncation mutants GST-DBD and GST-LBD, which respectively carry the DNA binding domain and the ligand binding domain containing the activating domain of AF-2 (**Fig. 2a**). The fluorescence intensity of GST-LBD, but not GST-DBD, was quenched with increasing amounts of Csn-B (**Fig. 2b**), but not Csn-C (**Supplementary Fig. 2c** online), which indicates that Csn-B physically interacts with the ligand binding domain. Given that molecular modeling and sequence alignment indicate that residue Tyr453 is conserved in the ligand binding pockets of many nuclear receptors[23–26] (**Fig. 1c**), we investigated whether the tyrosine residue plays a role in
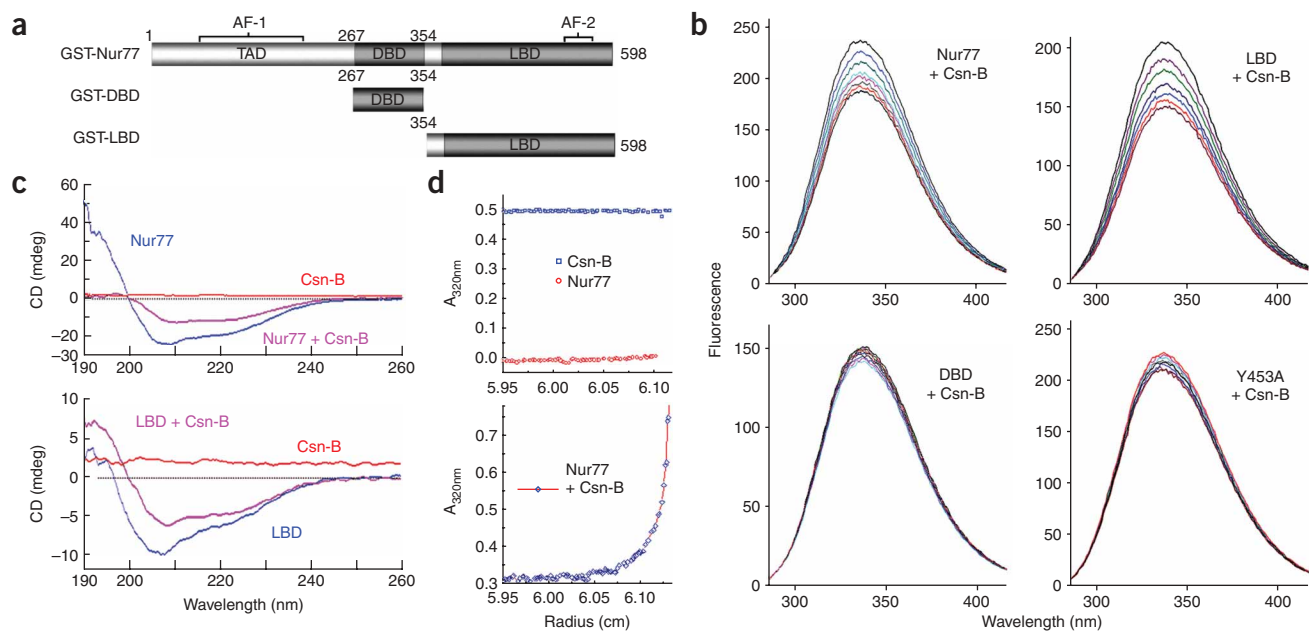
Figure 2 Csn-B physically binds to the ligand binding domain of Nur77. (**a**) Schematic representations of Nur77 and its truncation mutants. (**b**) Effect of Csn-B on fluorescence quenching of GST-Nur77 and its truncation and site mutants. Fluorescence spectra of GST-Nur77, and its truncation and site mutants (5 µM each), in the absence or presence of increasing amounts of Csn-B. (**c**,**d**) Analysis of Csn-B binding to Nur77 and its LBD by CD spectroscopy (**c**) and sedimentation equilibrium assay (**d**) as described in **Supplementary Methods**.

Csn-B binding. Indeed, Nur77 Y453A was no longer quenched in fluorescence emission by Csn-B at various concentrations (**Fig. 2b**). These data not only indicate that Csn-B interacts with the LBD of Nur77, but also suggest that Tyr453 is instrumental in Csn-B binding.

In addition, we also found that the fluorescence intensity decreased to a minimum as saturation of the GST-Nur77 protein or GST-LBD protein with Csn-B was achieved (**Supplementary Fig. 2d**), which may reflect specific binding of Csn-B to the ligand binding domain of Nur77. However, such an effect was not seen in GST-DBD or GST-Y453A (**Supplementary Fig. 2e**). To exclude the possibility that this quenching was caused by an inner filter effect, we used GST as a control. We observed only a marginal linear decrease of fluorescence that indicated inner filter (**Supplementary Fig. 2d**). When the fluorescence from inner filter was deducted, a corrected fluorescence intensity curve was obtained (**Supplementary Fig. 2d**). As a positive control, 9-*cis*-retinoic acid (9-*cis*-RA, **3**) binding resulted in fluorescence quenching of its receptor, RXRα protein (**Supplementary Fig. 2f**), as previously reported[27]. Moreover, plotting of the data from which the inner filter effect was deducted yielded titration curves for Nur77, LBD and RXRα, which we used in a previously described equation[28] to reach apparent dissociation constants (K_d) of 7.4×10^{-7} M and 1.51×10^{-6} M for Csn-B binding to Nur77 and LBD proteins, respectively (**Supplementary Fig. 2d**), and 2.4×10^{-7} M for 9-*cis*-RA binding to RXRα (**Supplementary Fig. 2f**). Importantly, the K_d of 9-*cis*-RA for RXRα that we obtained falls in the range of K_d values reported previously[27].

To further test whether Csn-B is a bona fide agonist for Nur77, we compared the quenching ability of Csn-B toward Nur77 to that of several other compounds that are known ligands for different nuclear receptors, including 9-*cis*-RA for retinoid receptors[13,29], 17-estradiol (E2, **4**) for estrogen receptor[30], rosiglitazone (**5**) for peroxisome proliferator–activated receptor γ (PPARγ)[31] and prostaglandin E2 (PGE2, **6**)[32]. As E2 and rosiglitazone were found to have an intrinsic

ability to emit fluorescence at a wavelength close to that for GST-Nur77 (336 nm) (**Supplementary Fig. 2a**), we discarded them and decided to use 9-*cis*-RA and PGE2. Surprisingly, 9-*cis*-RA and PGE2 both displayed quenching effects on Nur77, as did Csn-B (**Supplementary Fig. 2g,h**). However, whereas Csn-B failed to quench Y453A (**Fig. 1b**), the other ligands could still quench the mutant Y453A (**Supplementary Fig. 2g,h**). For example, the K_d values for 9-*cis*-RA binding to Nur77 and mutant Y453A were similar (7.2×10^{-7} M and 8.1×10^{-7} M, respectively; **Supplementary Fig. 2g,h**), which indicates that Csn-B and 9-*cis*-RA bind to separate sites.

We then used a biophysical approach to determine the binding affinity of Csn-B to Nur77. Surface plasmon resonance (BIAcore) was done to obtain the K_d for Csn-B binding to Nur77. The binding kinetics for Csn-B were estimated using global fitting analysis of the titration curves to the 1:1 Langmurian interaction model[33]. Csn-B bound GST-Nur77 with an ectodomain pattern (**Supplementary Fig. 2i**). The K_d for Csn-B binding to Nur77 was calculated to be 8.52×10^{-7} M based on the ratio of the dissociation rate constant (k_d, 7.01×10^{-3} s^{-1}) to the association rate constant (k_a, 8.23×10^{3} M^{-1} s^{-1}). In the control, no signal of ectodomain form for binding to GST appeared (**Supplementary Fig. 2i**). Csn-B binding to the ligand binding domain GST-LBD had kinetic constants of $k_d = 1.73 \times 10^{-2}$ s^{-1} and $k_a = 9.05 \times 10^{3}$ M^{-1} s^{-1}; the K_d was calculated to be 1.91×10^{-6} M. These values are comparable to those of the full-length of Nur77. These two K_ds were within the same range as those we obtained from quenching experiments, thus verifying the binding of Csn-B to Nur77 LBD. In contrast, Csn-B incubation with GST-DBD or GST-Y453A did not induce an ectodomain pattern (**Supplementary Fig. 2i**).

Finally, we performed a CD spectroscopic assay to determine whether Csn-B induces a conformational change in GST-Nur77. Csn-B, but not Csn-C, caused a change in the conformation of GST-Nur77 and GST-LBD (**Fig. 2c** and **Supplementary Fig. 2j**). In
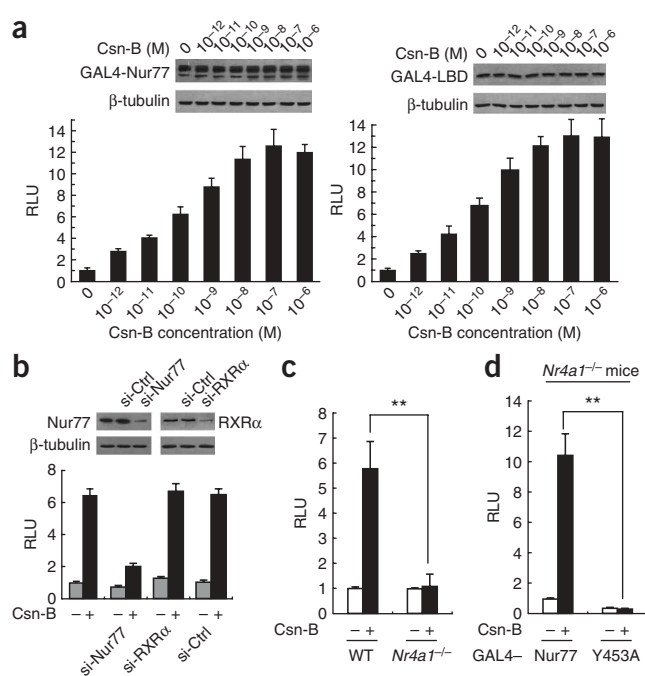
Figure 3 Csn-B activates Nur77 transactivational activity. (**a**) Csn-B stimulates the transactivational activity of GAL4-Nur77 and GAL4-LBD in BGC-823 cells. Insets show the expression levels of GAL4-Nur77 and GAL4-LBD in the transfected cells. BGC-823 cells were transfected with GAL4-Nur77 or GAL4-LBD, together with GAL4 reporter gene, and then treated with Csn-B for 12 h at different concentrations, as indicated. (**b**) Effect of siRNA against Nur77 or RXRα on Csn-B–induced transactivational activity. Cells were transfected with si-Nur77, si-RXRα or si-Ctrl (scrambled siRNA), together with NurRE-luciferase reporter and β-galactosidase expression vector. The expression levels of endogenous Nur77 and RXRα are shown in the insets. (**c**) Effect of Csn-B on Nur77 transactivational activity *in vivo*. Nur77, NurRE-luciferase reporter and β-galactosidase were mixed with an *in vivo* transfection reagent and injected into the tail vein of wild-type or *Nr4a1*^{−/−} mice (*n* = 5 for each group). After 5 h, mice were administered with vehicle (DMSO, 50 μl) or Csn-B (50 mg kg^{−1}) intraperitoneally. The luciferase activities in liver lysates were determined at 24 h post-injection. Data are presented as means ± s.e.m. ****P* < 0.01. (**d**) Nur77-Y453A is not activated by Csn-B. GAL4-Nur77 or GAL4-Y453A, GAL4-luciferase reporter genes, and β-galactosidase were transfected into *Nr4a1*^{−/−} mice (*n* = 5 for each group), and luciferase activities were determined (*P* < 0.01) as described for **Figure 3c**.

contrast, neither compound bound GST-DBD or GST-Y453A to induce a conformational change (**Supplementary Fig. 2j**), nor did addition of 9-*cis*-RA and PGE2 induce a conformational change in GST-LBD (**Supplementary Fig. 2k**), which further confirmed that these ligands do not have the same binding site as Csn-B. Sedimentation velocity analysis also indicated the binding of Csn-B with GST-Nur77 in solution (**Fig. 2d**). Taken together, these data led us to conclude that Csn-B specifically interacts with the ligand binding domain of Nur77, whereas other compounds bind to separate sites of the protein, as proposed.

Csn-B stimulates transactivational activity of Nur77

To delineate structural determinants of Nur77 in its response to Csn-B for transactivation, we first determined whether the ligand binding domain of Nur77 is required for Csn-B to stimulate its transcriptional activity by transfecting different truncated Nur77 constructs into BGC-823 cells. These cells were transfected with a chimeric GAL4-Nur77 (full-length Nur77), GAL4-DBD (DNA binding domain of Nur77 only), GAL4-LBD (ligand binding domain including an AF-2 region that has transactivation activity) or GAL4-Y453A, together with a reporter construct containing five GAL4 response elements linked to a luciferase reporter gene (pGAL4)[20]. The result showed that Csn-B induced luciferase activity in cells that were cotransfected with GAL4-Nur77 or GAL4-LBD (**Fig. 3a**), whereas no response was observed in cells that were cotransfected with GAL4-DBD or GAL4-Y453A (**Supplementary Fig. 3a** online). The EC$_{50}$ (the 50% effective concentration of Csn-B) values of Csn-B for Nur77 and LBD were 2.78×10^{-10} and 1.15×10^{-10} M, respectively (**Supplementary Fig. 3b**). In comparison, Csn-B had only a minimal effect on the transactivational activity of GAL4-Nurr1(LBD) and GAL4-NOR1(LBD) (**Supplementary Fig. 3c**). Furthermore, when 9-*cis*-RA and PGE2 were tested for their effect on the transactivational activity of Nur77, only Csn-B exhibited strong induction of Nur77 transactivational activity (**Supplementary Fig. 3d**). Taken together, these data support the notion that Csn-B targets the ligand binding domain of Nur77, which selectively stimulates the transactivational activity of Nur77.

To check whether Csn-B has any effect on the stability of the Nur77 protein, we determined the protein levels in the transfected cells. Results showed that the amount of GAL4-Nur77, GAL4-LBD, GAL4-DBD and GAL4-Y453A proteins were constant before and after Csn-B treatment (**Fig. 3a** and **Supplementary Fig. 3a**), thereby strongly suggesting that Csn-B indeed upregulates the transactivational activity of Nur77. To further explore the effect of Csn-B treatment on Nur77, we carried out an *in vitro* knockdown experiment by introducing expression vectors for small RNA (siRNA) against Nur77 or RXRα in gastric cancer cells BGC-823 (**Fig. 3b**). Csn-B–induced activity of the NurRE reporter gene was attenuated by siRNA against Nur77 by ∼three-fold below the siRNA control (scrambled siRNA), whereas siRNA against RXRα had no effect on the same reporter gene in the presence of Csn-B (**Fig. 3b**).

In addition, we analyzed the functional effect of Csn-B on the transactivation of Nur77 *in vivo* by carrying out *in vivo* hepatocyte transfection. In this experiment, wild-type and Nur77-null (*Nr4a1*^{−/−}) C57BL/6 mice were used. The luciferase reporter that is responsive to Nur77 was mixed with *in vivo* transfection reagent and injected into the tail vein of wild-type and *Nr4a1*^{−/−} mice. In the hepatocytes of wild-type mice, the transcriptional activity of the reporter was induced ∼five-fold with Csn-B treatment (**Fig. 3c**). However, in the *Nr4a1*^{−/−} mice, Csn-B failed to induce the same reporter, demonstrating a significant difference (*P* < 0.01) compared with the wild-type group (**Fig. 3c**). Similarly, in the *Nr4a1*^{−/−} mice, *in vivo* transfection of GAL4-Y453A did not promote the transcriptional activity of reporter gene in the presence of Csn-B, whereas wild-type Nur77 significantly (*P* < 0.01) induced the reporter activity in the presence of the agonist (**Fig. 3d**). Again, these results indicate that Csn-B specifically promotes transactivation of Nur77 *in vivo*.

Notably, we observed that *Nr4a1* mRNA levels were also upregulated by Csn-B treatment (**Supplementary Fig. 4a** online). Sequence analysis of the *Nr4a1* promoter revealed that it contains several potential monomeric Nur77 binding sites (NBREs) (**Supplementary Table 1** online), which infers the possibility of *Nr4a1* autoregulation of transcriptional activity. Electromobility shift assays (EMSA) showed that Nur77 bound to the *Nr4a1* promoter with a binding affinity comparable to the positive control elements NBRE or NurRE (dimeric Nur77 binding site) (**Fig. 4a**). The specificity of Nur77 binding to the promoter could also be seen by the observation that Nur77 could not
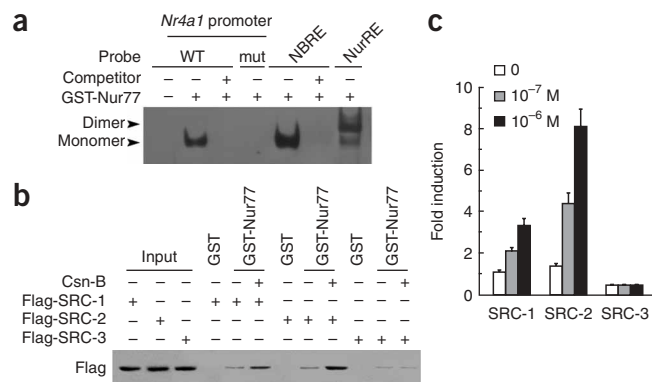
Figure 4 Csn-B mediates Nur77 autoregulation and cofactor recruitment. (**a**) EMSA of the *Nr4a1* promoter. GST-Nur77 proteins were incubated with biotin-labeled oligonucleotides that are NBRE elements present in the *Nr4a1* promoter, and with their mutant forms, along with a consensus NBRE and NurRE as positive controls (nucleotide sequences shown in **Supplementary Methods**). (**b**) Csn-B enhances interaction of Nur77 with SRCs, as detected by GST pull-down assay. GST-Nur77 or GST alone was incubated with cell lysates from 293T cells that were transfected with Flag-SRC-1, Flag-SRC-2 or Flag-SRC-3 and Csn-B (10^{-6} M) for 3 h. Inputs indicate relative expression levels of SRC proteins. (**c**) Effect of SRCs on Csn-B–induced Nur77 transactivation. BGC-823 cells were transfected with or without SRC-1, SRC-2 or SRC-3, NurRE-luciferase reporter and β-galactosidase, and were treated for 12 h with different concentrations of Csn-B. The fold induction was derived by comparing each luciferase activity to non-SRC transfection for a given concentration of Csn-B. All results are presented as means ± s.e.m.

bind to the promoter when its conserved elements were mutated (**Fig. 4a**). To more precisely define the binding motif in the promoter, we constructed several luciferase reporters containing the *Nr4a1* promoter of various lengths, including –500 to +22, –2,900 to +22, and –3,500 to +22 (pLuc-500, pLuc-2900 and pLuc-3500, respectively). Luciferase reporter assays showed that treatment of Csn-B stimulated the transcriptional activity of reporter genes pLuc-2900 and pLuc-3500 (which contains consensus Nur77 response elements), whereas Csn-B did not have any effect on pLuc-500, which did not carry the Nur77 binding site (**Supplementary Fig. 4b**). Thus, Csn-B exerts its effect on Nur77 mRNA levels at least partially through positive autoregulation.

Previous studies demonstrated that Nur77 requires coactivators such as SRC-1 and SRC-2 (steroid receptor coactivators) for the transactivation of target genes[34,35]. GST pull-down assays indicated that Nur77 interacts with SRC-1, SRC-2 and weakly with SRC-3 in 293T cells, and that Csn-B treatment enhances Nur77 association with SRC-2 and SRC-1, but not with SRC-3 (**Fig. 4b**). We then investigated whether an Csn-B–activated Nur77-SRC association promotes the recruitment of the coactivators to Nur77 response elements. To this end, we performed chromatin immunoprecipitation (ChIP) assays using NurRE as a probe and analyzed the recruitment of SRC cofactors. Csn-B recruited SRC-2 and to a lesser extent SRC-1, but not SRC-3, to NurRE (**Supplementary Fig. 4c**). SRC-2 and SRC-1 consistently enhanced the transactivational activity of Nur77, which was further stimulated by Csn-B in a dose-dependent manner (**Fig. 4c**). Together, these data indicate that the transactivational activity of Nur77 is activated by Csn-B, which also promotes recruitment of the coactivators SRC-2 and SRC-1.

Csn-B increases blood glucose levels
Nur77 increases blood glucose concentrations by enhancing gluconeogenic gene expression[14]. If Csn-B is a genuine agonist for Nur77, it is expected that Csn-B would also elicit such an effect on blood glucose levels (**Fig. 5**). To analyze the biological function of Csn-B in Nur77-mediated regulation of glucose levels, we tested the levels of blood glucose in wild-type and $Nr4a1^{-/-}$ mice. Csn-B significantly ($P < 0.01$) changed blood glucose levels in fasting wild-type mice (**Fig. 5a**). In wild-type mice, after fasting for 16 h, the basal levels of blood glucose declined to 3.2 mM. However, Csn-B treatment significantly increased glucose levels from 3.2 to 11.4 mM ($P < 0.01$) within the first 30 min, and thereafter blood glucose gradually decreased before reaching the initial level after 300 min (**Fig. 5a**). By contrast, in $Nr4a1^{-/-}$ mice Csn-B induced a diminished increase in glucose levels within the first 30 min (from 3.7 to 5.8 mM) as compared with the wild type, which was close to the effect of control injections (**Supplementary Fig. 5a** online).

Multiple genes that participate in the gluconeogenic and glycolytic pathways are induced by Nur77 overexpression in mouse hepatocytes and skeletal muscle[14,36]. Given that Nur77 affects gluconeogenesis and glycolysis, we hypothesized that Csn-B may regulate related genes in these two pathways mediated by Nur77. To test this hypothesis, we chose several genes for real-time PCR analysis, including the genes encoding glucose-6-phosphatase (*G6pc*) and fructose-1,6-bisphophatase (*Fbp1*) for the gluconeogenesis pathway, and the genes encoding hexokinase (*Hk*), phosphofructokinase (*Pfk*) and pyruvate kinase (*Pk*) for the glycolysis pathway[14]. Cellular mRNA was prepared from the livers of wild-type and $Nr4a1^{-/-}$ mice that were treated with Csn-B. We observed after 30 min of Csn-B treatment that expression significantly ($P < 0.01$) increased for *G6pc* (4.1-fold) and *Fbp1* (3.0-fold), as compared with the control (**Fig. 5c**). Concomitant with the glucose level changes, 300 min after administration of Csn-B, the expression levels of these genes returned to initial levels (**Fig. 5c**). However, we did not observe any change in gene expression of *Hk*, *Pfk* or *Pk* after 30 to 300 min of Csn-B treatment in wild-type mice (**Fig. 5c**). Importantly, the Csn-B effect on the glucogenic genes was not observed in $Nr4a1^{-/-}$ mice (**Supplementary Fig. 5b**). These results indicate that Csn-B only influences gluconeogenesis, and that Csn-B depends on Nur77 to exert changes in this pathway.

As insulin acts to reduce blood glucose levels and Csn-B elevates blood glucose levels, we next investigated whether Csn-B has an antagonistic effect on insulin. As expected, a ~three-fold reduction of glucose levels in insulin-treated mice occurred within 30 min (**Fig. 5b**). However, in the mice treated with insulin and Csn-B together, Csn-B was able to abrogate the decline of glucose levels caused by insulin administration. Quantitative real-time PCR showed an increase in *G6pc* and *Fbp1* expression in liver of 6.23- and 3.05-fold, respectively, in insulin plus Csn-B treatment after 60 min (**Supplementary Fig. 5c**). Therefore, the expression patterns of the gluconeogenic genes correlate with the glucose concentration changes in mice cotreated with Csn-B and insulin.

Csn-B induces apoptosis by targeting Nur77 to mitochondria
Next we tested for the ability of Csn-B to induce apoptosis *in vitro* in cancer cells given that Nur77 is implicated in induction of apoptosis[11,12,37]. Indeed, Csn-B displayed robust pro-apoptotic activity in gastric cancer cells BGC-823. We observed 63.5% of the cells to be apoptotic when treated with Csn-B for 48 h (**Fig. 6a**). Induction of apoptosis by Csn-B was closely related to Nur77 activity, as introduction of siRNA against Nur77 into BGC-823 cells resulted in a ~2.5-fold reduction in Csn-B–induced apoptosis (20.1%) as compared with the siRNA control (56.3%) (**Fig. 6a**). The Csn-B–induced
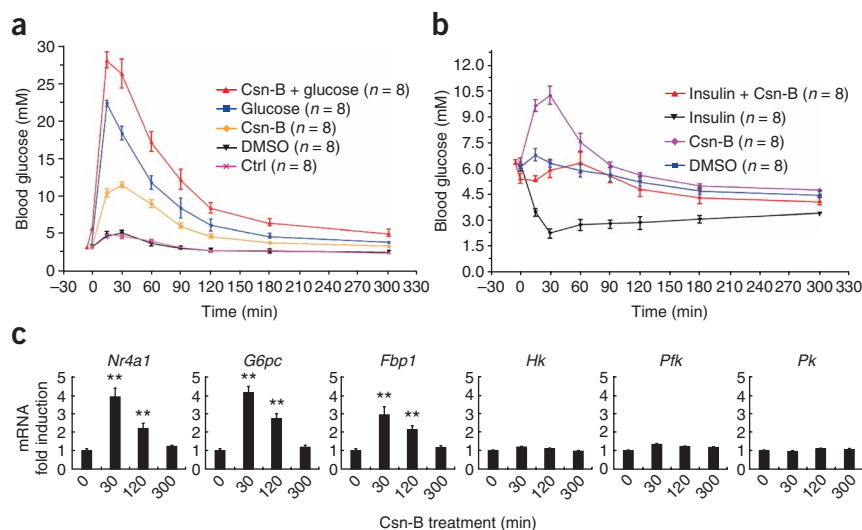
Figure 5 Csn-B increases blood glucose levels and expression of gluconeogenic genes. (**a,b**) Effect of Csn-B on blood glucose levels in wild-type mice. Wild-type mice were fasted for 16 h before Csn-B (50 mg kg^{-1}) or glucose (2 g kg^{-1}) injection (**a**), or for 5 h before insulin (0.5 U kg^{-1}) injection (**b**). Glucose levels were recorded at different times as indicated. DMSO (50 μl) was used as a vehicle control. Control group refers to the mice that received only an injection without any vehicle. (**c**) Effect of Csn-B on mRNA expression levels of gluconeogenic and glycolytic genes. Livers of mice were dissected at different times indicated after administration of Csn-B. Total RNA was prepared, and the mRNA levels of different genes were analyzed by real-time PCR. The fold induction was plotted against the DMSO treatment for all given time points. All results are presented as means ± s.e.m. Representatives of two independent experiments with similar results are shown. **P < 0.01.

apoptotic cells displayed characteristic nuclear DNA condensation (**Supplementary Fig. 6a** online), resulting in cytochrome *c* release and caspase-9 cleavage (**Supplementary Fig. 6b**). However, Csn-C did not induce apoptosis (**Supplementary Fig. 6c**) or release of cytochrome *c* (**Supplementary Fig. 6d**) in BGC-823 cells.

Several lines of recent evidence suggest that Nur77-mediated apoptosis is associated with Nur77 nucleocytoplasmic translocation accompanied by transcriptional regulation[11–13,37]. Therefore, we examined the subcellular localization of Nur77 in response to Csn-B stimulation using confocal microscopy. To establish a baseline, a GFP-Nur77 fusion construct was transfected into BGC-823 cells to test the subcellular location of Nur77. GFP-Nur77 was found in the mitochondria of about 70% of cells with treatment of Csn-B. In contrast, without Csn-B addition, Nur77 was exclusively localized in the nucleus of more than 90% of cells (**Fig. 6b**). Addition of Csn-B, but not of Csn-C, induced nuclear export of endogenous Nur77 in BGC-823 cells; however, such nucleocytoplasmic translocation was blocked by leptomycin B (LMB, **7**), a specific inhibitor of nuclear protein export (**Fig. 6c**). After LMB treatment, Csn-B was able to promote

translocation of Nur77 to the cytoplasm in only approximately 15% of transfected cells (**Supplementary Fig. 6e**). Mutation at Tyr453 in Nur77 resulted in the loss of translocation in the presence of Csn-B; almost no cytoplasmic localization of Nur77 was observed (**Supplementary Fig. 6f**). Together, these results suggest that Csn-B induces Nur77-mediated apoptosis through relocalization of Nur77 from the nucleus to the mitochondria.

Csn-B inhibits cancer cell proliferation and tumor growth

The apoptotic action of Csn-B via its binding to Nur77 prompted us to further investigate the anticancer activity of Csn-B with *in vitro* proliferation assays and *in vivo* by examining growth repression of xenograft tumors in nude mice. MTT (3-(4,5-dimethyl-2-thiazolyl)-2,5-diphenyltetrazolium bromide) assays indicated that Csn-B inhibited proliferation of human gastric cancer BGC-823 cells and human colon cancer SW620 cells by >70% (**Fig. 7a**), but it had a modest effect on human lung cancer H1299 cells and human hepatoma HepG2 cells (inhibition ≥ 40%) and a small effect on mouse NIH3T3 fibroblasts, human normal liver HL-7702 cells and ME-Hep4

Figure 6 Csn-B induces apoptosis via Nur77 in BCG-823 cells. (**a**) Induction of apoptosis by Csn-B. Cells were transfected with or without si-Nur77 and si-Ctrl (scrambled siRNA) as indicated, and then treated with Csn-B (5 μg ml^{-1}) for 48 h. Apoptotic cells were determined by flow cytometry assay. (**b**) Nur77 was translocated to the mitochondria upon Csn-B treatment. GFP-Nur77–transfected cells were treated with Csn-B (5 μg ml^{-1}) for 12 h, then immunostained with anti-Hsp60 followed by Texas Red–conjugated antibody. Nur77 protein was visualized under a confocal microscope. Scale bar, 10 μm. (**c**) Translocation of Nur77 from the nucleus to the cytoplasm in response to Csn-B or Csn-C. Cells were pretreated with or without LMB (1 ng ml^{-1}) for 3 h, followed by Csn-B or Csn-C (5 μg ml^{-1} each) for an additional 12 h. Endogenous Nur77 was stained with anti-Nur77 antibody, followed by fluorescein isothiocyanate (FITC)-conjugated antibody. Finally, the nuclei were stained with 4′,6-diamidino-2-phenylindole (DAPI). Scale bar, 10 μm.
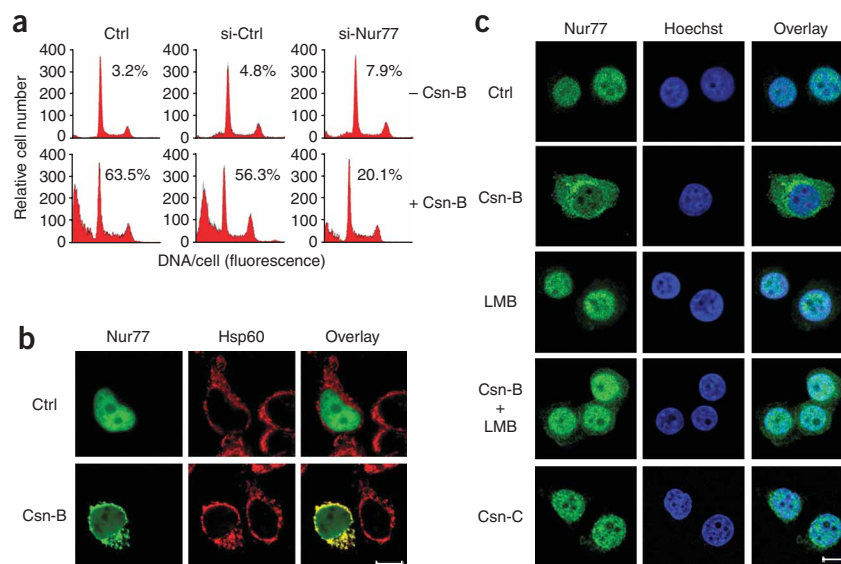
Figure 7 Csn-B inhibits growth of cancer cells and xenograft tumors. (**a**) Csn-B inhibits growth of cancer cells. Human gastric cancer BGC-823 cells and human colon cancer SW620 cells were treated with Csn-B for 72 h at various concentrations, as indicated. The number of viable cells was determined by MTT assay. (**b**) Csn-B effects on the growth of xenograft tumors in nude mice that were injected with three different BGC-823 cells, including BGC-823 cells expressing endogenous wild-type Nur77 (Nur77-WT), BGC-823 cells with $Nr4a1^{-/-}$ knocked down by its siRNA (si-Nur77), and BGC-823 cells with Nur77 mutated in its siRNA sequence (si-Ctrl). Nude mice were administered with Csn-B as described in the Methods. The xenograft tumors of various sizes are shown. Scale bar, 1 cm. (**c**) Subcellular localization of Nur77 in the specimens of xenograft tumors. Immunohistochemistry experiments were carried out to reveal the localization of Nur77 protein in the three kinds of tumor samples in the non-Csn-B treatment and Csn-B treatment groups. Scale bar, 30 μm. (**d**) Apoptotic cells were identified by TUNEL assay in specimens of xenograft tumors from nude mice as indicated in **b**. Scale bar, 100 μm.
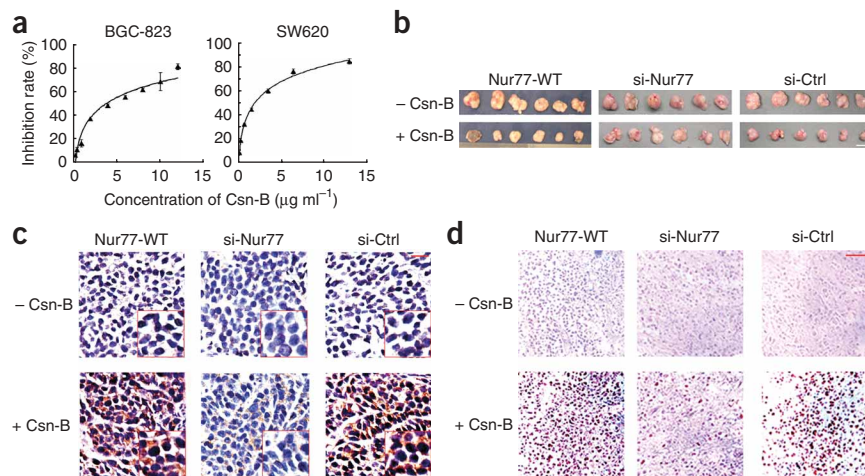
hepatoblasts from mouse E13.5 liver (**Supplementary Fig. 6g**). These results indicate a selective effect of Csn-B on cancerous cells.

In vivo determination of the antitumor effect of Csn-B was carried out by injecting gastric cancer cells BGC-823 subcutaneously into nude mice ($n = 6$). One week later, Csn-B was administered intraperitoneally to the recipient nude mice at a dosage of 13 mg kg^{-1} twice a week. Four weeks after starting Csn-B administration, tumors were removed to determine the weight. In parallel, we established two BGC-823 cell sublines that separately express siRNA against Nur77 (si-Nur77) and a control siRNA (si-Ctrl) containing alterations in two nucleotides compared with si-Nur77. These two sublines were also injected into nude mice, and the xenografts were analyzed. As summarized in **Table 1** and **Figure 7b**, in normal BGC-823–injected mice (labeled as Nur77-WT), tumor growth was significantly reduced with Csn-B treatment (41.6% inhibition in weight, $P < 0.05$). However, Csn-B did not inhibit tumor growth in mice injected with si-Nur77 cells (10.2% inhibition, $P > 0.05$) as compared with mice injected with si-Ctrl cells (43.6% inhibition, $P < 0.05$). Importantly, the nude mice did not display any discomfort or discernible side effects in diet intake or overall body weight during administration of Csn-B.

To further verify the effects of Csn-B on Nur77 function in the xenograft tumors, we carried out western blots and immunohistochemistry to examine Nur77 expression and localization, as well as TUNEL (terminal dUTP nick end labeling) assays to detect apoptotic cells on tissue sections of the xenograft tumors. We found that mice injected with Nur77-WT (BGC-823) cells or si-Ctrl–expressing cells

contained increased Nur77 protein levels after Csn-B administration (**Fig. 7c** and **Supplementary Fig. 6h**). Csn-B administration also increased the total number of apoptotic cells in xenograft tumors derived from BGC-823 cells and from si-Ctrl–expressing cells, but not from si-Nur77–expressing cells (**Fig. 7d**). In the specimens injected with BGC-823 cells, we also noted that Nur77 was present in both the nuclei and cytoplasm in the Csn-B–treated group, but was present predominantly in the nuclei of the non-Csn-B–treated group (**Fig. 7c**), which is in accordance with the results obtained from cell treatment experiments. In contrast, Nur77 protein displayed predominant nuclear localization in mice injected with si-Nur77 cells in both Csn-B–treated and non-Csn-B–treated samples, whereas both nuclear and cytoplasmic localization in mice injected with si-Ctrl cells was observed in Csn-B–treated samples but not in non-Csn-B–treated samples (**Fig. 7c**). Together, these data agree with our *in vitro* observations; they indicate that Csn-B induces *Nr4a1* expression by autoregulation *in vivo* and that Csn-B causes translocation of Nur77 from the nucleus to the cytoplasm to induce apoptosis in tumor tissue, thereby inhibiting tumor growth.

DISCUSSION
Despite the fact that the orphan receptor Nur77 is linked to various important biological functions[11,14,29,38,39], no physiological ligand is known. In this study, we identified Csn-B, an octaketide, as an agonist for Nur77. We found that Csn-B physically binds to Nur77 and subsequently activates its transactivational activity and translocation

Table 1 Effect of Csn-B on repression of tumors in nude mice

| Nude mice | Rate of tumor occurrence (%) | Mean weight of mice | | Mean weight of tumor | Inhibition (%) |
		Before treatment	After treatment		
Nur77-WT; Ctrl	100 (6/6)	15.21 ± 1.81	21.96 ± 1.62	1.86 ± 0.34	41.6 ($P = 0.003$)
Nur77-WT; Csn-B	100 (6/6)	15.81 ± 1.62	20.31 ± 1.73	1.09 ± 0.26	
si-Nur77; Ctrl	100 (6/6)	15.35 ± 1.21	20.98 ± 1.50	1.77 ± 0.27	10.2 ($P = 0.251$)
si-Nur77; Csn-B	100 (6/6)	15.63 ± 1.42	20.52 ± 1.33	1.59 ± 0.20	
si-Ctrl; Ctrl	100 (6/6)	16.50 ± 2.01	22.34 ± 1.92	1.95 ± 0.26	43.6 ($P = 0.002$)
si-Ctrl; Csn-B	100 (6/6)	16.22 ± 2.13	20.87 ± 1.89	1.10 ± 0.20	

All data are presented as means ± s.d.

to mitochondria to induce apoptosis. Further evidence that Csn-B is an agonist of Nur77 was derived from fluorescence quenching assays, circular dichroism measurement and BIAcore analysis. We have also suggested biological functions of Csn-B in glucose metabolism. Importantly, these functions of Csn-B all agree with the functions previously identified for Nur77 (refs. 11,14,36,38,40). Moreover, we have shown that Csn-B depends on Nur77 to selectively activate the NurRE reporter gene.

Analysis of the crystal structures of mouse Nurr1 LBD and the *Drosophila* NOR1 homolog DHR38 (refs. 17–19), and the structure of Nur77, reveals a potential ligand binding pocket in their LBD. Inside this pocket, there is a tyrosine residue that is conserved among many nuclear receptors[23–26] and is located at position 453 in Nur77. Fluorescence quenching experiments showed that Csn-B quenches the fluorescence of wild-type Nur77, but not the Y453A mutant, which indicates that the conserved tyrosine residue may form a contact with Csn-B or that Csn-B binding to the pocket may somehow cause a conformational change that in turn influences the fluorescence emission of Tyr453. The importance of Tyr453 was further underscored by our *in vivo* reporter assay, which showed that the wild-type Nur77 but not the mutant Y453A could be induced by Csn-B to activate the reporter gene.

Another aspect of functional resemblance of Csn-B to Nur77 is that Csn-B administration leads to an acute boost of blood glucose levels in fasting C57 mice. A recent study showed that overexpression of Nur77 by an adenoviral expression system in mice results in enhanced activity of gluconeogenesis, which is manifested by increased blood glucose levels and increased expression of gluconeogenic enzymes encoded by *G6pc* and *Fbp1* (ref. 14). We demonstrated that Csn-B treatment in wild-type fasting mice could increase blood glucose levels, and gluconeogenic genes such as *G6pc* and *Fbp1* were all induced by Csn-B in the liver tissue of mice. Moreover, we demonstrated that in *Nr4a1*$^{-/-}$ mice, Csn-B did not induce the expression of the gluconeogenic genes or cause an increase of blood glucose levels, thereby providing an important line of genetic evidence indicating that Csn-B elicits biological functions through its receptor Nur77.

In summary, our work demonstrates that Csn-B is a bona fide agonist for Nur77. The availability of this natural product will open new avenues for studying the orphan receptor Nur77. Importantly, Csn-B may represent a new candidate or lead compound for cancer treatment and for treating individuals with hypoglycemia.

METHODS

Isolation and characterization of cytosporone B and cytosporone C. Csn-B and Csn-C were purified from the mycelia of the endophytic fungal strain *Dothiorella* sp. HTF3, which was isolated from mangrove trees and cultured in liquid potato dextrose broth medium. The structures of these compounds were determined by NMR (**Supplementary Table 2** online), and antimicrobial activities were determined against several species (**Supplementary Table 3** online). For more detailed information on fungal fermentation, chemical extraction and structural determination of the compounds, see **Supplementary Methods** online.

Molecular modeling. The three-dimensional geometry data file for Nur77 was obtained from the Protein Data Bank. Three-dimensional geometry for Csn-B was created and optimized using the computational chemistry package Ghemical[41] with 0.001 gradient cutoff and 1×10^{-7} δ E cutoff. AutoDock3.0 (ref. 42) and AutoDockTools (http://autodock.scripps.edu/resources/) were used to investigate Csn-B binding to Nur77. The search was based on a Lamarckian genetic algorithm. Default values were selected for Docking Searching Parameter and Docking Run Parameters. DS Modeling 1.1 (Accelrys) was used to generate images of Csn-B and Nur77.

Tumor xenograft experiment. Athymic nude mice (BALB/c, SPF grade, ~16 g, four weeks old) were housed in a laminar flow under sterilized conditions. The temperature was maintained at 28 °C. Mice were fed with autoclaved mouse chow. The inoculation dosage with BGC-823 cells was 0.05 ml of cell suspension per mouse (cell density was 2.5×10^{10} l^{-1}). Different cells, including wild-type BGC-823 cells and BGC-823 cells separately expressing si-Nur77 and si-Nur77-ctrl, were injected subcutaneously into nude mice. The inoculated mice were randomly separated into two groups. One group was given an injection to the abdominal cavity at a dosage of 13 mg kg^{-1} of Csn-B (one tenth of the dosage lethal to 50% of mice tested (LD$_{50}$)) twice a week. The other group was administered with the same dissolvent (DMSO) without Csn-B. Food consumption and body weight of nude mice were monitored weekly. Four weeks later, the nude mice were killed and the tumors formed were removed, fixed and embedded. All results were presented as means ± s.d. *P* value was determined by a two-tailed Student's *t*-test.

Blood glucose test. Wild-type and *Nr4a1*$^{-/-}$ C57BL/6 mice (six weeks old) were fasted, with water supply, for 16 h (for glucose tolerance test) or 5 h (for insulin tolerance test) before blood sampling through the tail vein. Mice were then injected intraperitoneally with Csn-B at a dosage of 50 mg kg^{-1}. Injections with glucose (2 g kg^{-1}), insulin (0.5 U kg^{-1}) or DMSO (50 μl), even without any vehicle, were used as controls. Blood glucose levels were measured at 15, 30, 60, 90, 120, 180 and 300 min after treatment, using a OneTouch Ultra glucometer (Lifescan). The weights of mice were recorded before every test. All data are presented as means ± s.e.m. The experiments were carried out in the Cancer Research Center of Xiamen University under the guidelines of the Xiamen University Institutional Animal Care and Use Committee.

Other methods. Details for other methods, including cell culture, plasmid construction, luciferase assay, fluorescence quench assay, BIAcore analysis, sedimentation equilibrium study, CD spectroscopy, transient transfection, western blot, apoptosis assay, RT-PCR, real-time PCR, EMSA, ChIP assay, MTT assay and isolation and structure elucidation of Csn-B and Csn-C, are provided in the **Supplementary Methods**.

Accession codes. Protein Data Bank: The crystal structure of Nur77 was deposited as part of a previous study under accession code 2QW4.

Note: Supplementary information and chemical compound information is available on the Nature Chemical Biology website.

AUTHOR CONTRIBUTIONS
Q.W., Y.S. and S.-C.L. designed experiments and wrote the manuscript. S.-C.L.'s group (Q.L., S.S., S.L., Z.Y. and D.H.) performed molecular experiments; Y.S.'s group (X.D., Q.X., Z.Z., Y.H. and W.S.) performed isolation, identification and preparation of Csn-B and Csn-C; B.C.W.'s group (D.C. and Z.C.) performed molecular modeling; Q.W.'s group (Y.Z., H.C., J.L., B.Z., L.Z., G.L. and M.Z.) performed the rest of the experiments.

Published online at http://www.nature.com/naturechemicalbiology/
Reprints and permissions information is available online at http://npg.nature.com/reprintsandpermissions/

1. Giguere, V. Orphan nuclear receptors: from gene to function. *Endocr. Rev.* **20**, 689–725 (1999).
2. Winoto, A. & Littman, D.R. Nuclear hormone receptors in T lymphocytes. *Cell* **109** Suppl: S57–S66 (2002).
3. Nuclear Receptors Nomenclature Committee. A unified nomenclature system for the nuclear receptor superfamily. *Cell* **97**, 161–163 (1999).

4. Germain, P., Staels, B., Dacquet, C., Spedding, M. & Laudet, V. Overview of nomenclature of nuclear receptors. *Pharmacol. Rev.* **58**, 685–704 (2006).
5. Philips, A. *et al.* Novel dimeric Nur77 signaling mechanism in endocrine and lymphoid cells. *Mol. Cell. Biol.* **17**, 5946–5951 (1997).
6. Wilson, T.E., Fahrner, T.J., Johnston, M. & Milbrandt, J. Identification of the DNA binding site for NGFI-B by genetic selection in yeast. *Science* **252**, 1296–1300 (1991).
7. Liu, Z.G., Smith, S.W., McLaughlin, K.A., Schwartz, L.M. & Osborne, B.A. Apoptotic signals delivered through the T-cell receptor of a T-cell hybrid require the immediate-early gene nur77. *Nature* **367**, 281–284 (1994).
8. Woronicz, J.D., Calnan, B., Ngo, V. & Winoto, A. Requirement for the orphan steroid receptor Nur77 in apoptosis of T-cell hybridomas. *Nature* **367**, 277–281 (1994).
9. Cheng, L.E., Chan, F.K., Cado, D. & Winoto, A. Functional redundancy of the Nur77 and Nor-1 orphan steroid receptors in T-cell apoptosis. *EMBO J.* **16**, 1865–1875 (1997).
10. Kagaya, S. *et al.* NR4A orphan nuclear receptor family in peripheral blood eosinophils from patients with atopic dermatitis and apoptotic eosinophils in vitro. *Int. Arch. Allergy Immunol.* **137** (suppl. 1): 35–44 (2005).
11. Li, H. *et al.* Cytochrome c release and apoptosis induced by mitochondrial targeting of nuclear orphan receptor TR3. *Science* **289**, 1159–1164 (2000).
12. Wu, Q., Liu, S., Ye, X.F., Huang, Z.W. & Su, W.J. Dual roles of Nur77 in selective regulation of apoptosis and cell cycle by TPA and ATRA in gastric cancer cells. *Carcinogenesis* **23**, 1583–1592 (2002).
13. Lin, X.F. *et al.* RXRalpha acts as a carrier for TR3 nuclear export in a 9-cis retinoic acid-dependent manner in gastric cancer cells. *J. Cell Sci.* **117**, 5609–5621 (2004).
14. Pei, L. *et al.* NR4A orphan nuclear receptors are transcriptional regulators of hepatic glucose metabolism. *Nat. Med.* **12**, 1048–1055 (2006).
15. Fu, Y., Luo, L., Luo, N., Zhu, X. & Garvey, W.T. NR4A orphan nuclear receptors modulate insulin action and the glucose transport system: potential role in insulin resistance. *J. Biol. Chem.* **282**, 31525–31533 (2007).
16. Mangelsdorf, D.J. & Evans, R.M. The RXR heterodimers and orphan receptors. *Cell* **83**, 841–850 (1995).
17. Baker, K.D. *et al.* The *Drosophila* orphan nuclear receptor DHR38 mediates an atypical ecdysteroid signaling pathway. *Cell* **113**, 731–742 (2003).
18. Wang, Z. *et al.* Structure and function of Nurr1 identifies a class of ligand-independent nuclear receptors. *Nature* **423**, 555–560 (2003).
19. Flaig, R., Greschik, H., Peluso-Iltis, C. & Moras, D. Structural basis for the cell-specific activities of the NGFI-B and the Nurr1 ligand-binding domain. *J. Biol. Chem.* **280**, 19250–19258 (2005).
20. Chintharlapalli, S. *et al.* Activation of Nur77 by selected 1,1-Bis(3′-indolyl)-1-(p-substituted phenyl)methanes induces apoptosis through nuclear pathways. *J. Biol. Chem.* **280**, 24903–24914 (2005).
21. Cho, S.D. *et al.* Nur77 agonists induce proapoptotic genes and responses in colon cancer cells through nuclear receptor-dependent and nuclear receptor-independent pathways. *Cancer Res.* **67**, 674–683 (2007).
22. Brady, S.F., Wagenaar, M.M., Singh, M.P., Janso, J.E. & Clardy, J. The cytosporones, new octaketide antibiotics isolated from an endophytic fungus. *Org. Lett.* **2**, 4043–4046 (2000).
23. Nolte, R.T. *et al.* Ligand binding and co-activator assembly of the peroxisome proliferator-activated receptor-gamma. *Nature* **395**, 137–143 (1998).
24. Ray, D.W., Suen, C.S., Brass, A., Soden, J. & White, A. Structure/function of the human glucocorticoid receptor: tyrosine 735 is important for transactivation. *Mol. Endocrinol.* **13**, 1855–1863 (1999).
25. Agostini, M. *et al.* Tyrosine agonists reverse the molecular defects associated with dominant-negative mutations in human peroxisome proliferator-activated receptor gamma. *Endocrinology* **145**, 1527–1538 (2004).
26. Koehler, K.F., Helguero, L.A., Haldosen, L.A., Warner, M. & Gustafsson, J.A. Reflections on the discovery and significance of estrogen receptor beta. *Endocr. Rev.* **26**, 465–478 (2005).
27. Chen, Z.P. *et al.* Pure and functionally homogeneous recombinant retinoid X receptor. *J. Biol. Chem.* **269**, 25770–25776 (1994).
28. Cogan, U., Kopelman, M., Mokady, S. & Shinitzky, M. Binding affinities of retinol and related compounds to retinol binding proteins. *Eur. J. Biochem.* **65**, 71–78 (1976).
29. Wu, Q. *et al.* Modulation of retinoic acid sensitivity in lung cancer cells through dynamic balance of orphan receptors nur77 and COUP-TF and their heterodimerization. *EMBO J.* **16**, 1656–1669 (1997).
30. Cheskis, B.J., Karathanasis, S. & Lyttle, C.R. Estrogen receptor ligands modulate its interaction with DNA. *J. Biol. Chem.* **272**, 11384–11391 (1997).
31. Pavan, L. *et al.* Human invasive trophoblasts transformed with simian virus 40 provide a new tool to study the role of PPARgamma in cell invasion process. *Carcinogenesis* **24**, 1325–1336 (2003).
32. Najarian, T. *et al.* Preservation of neural function in the perinate by high PGE(2) levels acting via EP(2) receptors. *J. Appl. Physiol.* **89**, 777–784 (2000).
33. Cain, S.A. *et al.* Fibrillin-1 interactions with heparin. Implications for microfibril and elastic fiber assembly. *J. Biol. Chem.* **280**, 30526–30537 (2005).
34. Maira, M., Martens, C., Batsche, E., Gauthier, Y. & Drouin, J. Dimer-specific potentiation of NGFI-B (Nur77) transcriptional activity by the protein kinase A pathway and AF-1-dependent coactivator recruitment. *Mol. Cell. Biol.* **23**, 763–776 (2003).
35. Wansa, K.D., Harris, J.M. & Muscat, G.E. The activation function-1 domain of Nur77/NR4A1 mediates trans-activation, cell specificity, and coactivator recruitment. *J. Biol. Chem.* **277**, 33001–33011 (2002).
36. Chao, L.C. *et al.* Nur77 coordinately regulates expression of genes linked to glucose metabolism in skeletal muscle. *Mol. Endocrinol.* **21**, 2152–2163 (2007).
37. Kolluri, S.K. *et al.* Mitogenic effect of orphan receptor TR3 and its regulation by MEKK1 in lung cancer cells. *Mol. Cell. Biol.* **23**, 8651–8667 (2003).
38. Lin, B. *et al.* Conversion of Bcl-2 from protector to killer by interaction with nuclear orphan receptor Nur77/TR3. *Cell* **116**, 527–540 (2004).
39. Wu, Q. *et al.* Inhibition of trans-retinoic acid-resistant human breast cancer cell growth by retinoid X receptor-selective retinoids. *Mol. Cell. Biol.* **17**, 6598–6608 (1997).
40. Mullican, S.E. *et al.* Abrogation of nuclear receptors Nr4a3 and Nr4a1 leads to development of acute myeloid leukemia. *Nat. Med.* **13**, 730–735 (2007).
41. Hassinen, T. & Peräkylä, M. New energy terms for reduced protein models implemented in an off-lattice force field. *J. Comput. Chem.* **22**, 1229–1242 (2001).
42. Morris, G.M. *et al.* Automated docking using a Lamarckian genetic algorithm and an empirical binding free energy function. *J. Comput. Chem.* **19**, 1639–1662 (1998).